# Supplementary material

# NiCoP/g-$C_3N_4$ Nanocomposites for Efficient Photocatalytic Hydrogen Production from Seawater

Zhufeng Lu[a,b†], Qiaoyi Xiao[a,d†], Yangjie Zhou[a], Li Zhou[a], Qiqi Gu[a], Yuan Lian[a,d], Hongmei Wang[a,*], Siqian Zhang[a], Xiao Wang[c,*]

[a] *College of Biological, Chemical Sciences and Engineering, Jiaxing University, Jiaxing 314001, China*

[b] *Analytical & Testing Center, Jiaxing University, Jiaxing 314001, China*

[c] *School of Physics, East China University of Science and Technology, Shanghai 200237, China*

[d] *College of Material and Textile Engineering, Jiaxing University, Jiaxing 314001, China*

## 1. Experimental

### 1.1 Synthesis of g-$C_3N_4$

A mixture of 5.0 g melamine and 1.0 g ammonium oxalate monohydrate was thoroughly ground to ensure uniform blending. The resulting mixture was placed in an alumina crucible and heated in static air at a ramp rate of 3 °C/min to 550 °C, where it was maintained for 4 h. After thermal treatment, a yellow bulk precursor was obtained, which was then ground into a fine powder and transferred into a 150 mL beaker. Deionized water was added, and the suspension was subjected to ultrasonic treatment for 7 h to yield well-dispersed g-$C_3N_4$ nanosheets. The resulting suspension was subsequently washed three times with distilled water and absolute ethanol to remove unreacted species and exfoliation residues. Finally, the suspension was dried at 70 °C for 12 h to obtain the g-$C_3N_4$ nanosheets.

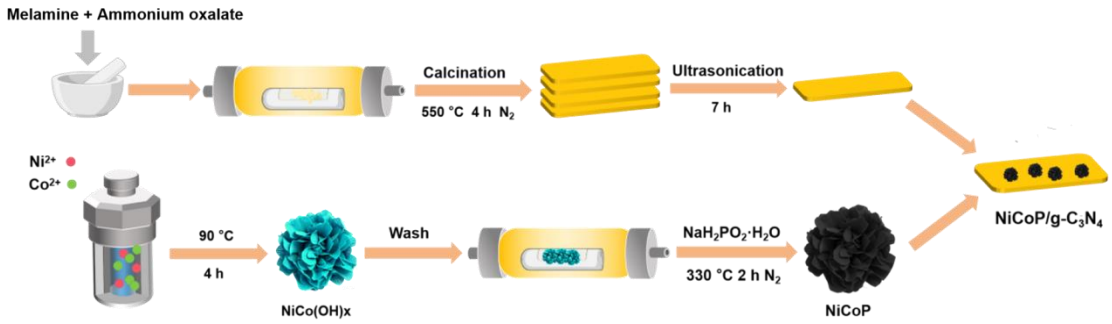


Figure S1 The synthesis route of NiCoP/g-$C_3N_4$ Nanocomposites.

* Corresponding author: (E-mail: hongmei256@163.com (H. Wang); laricswang@ecust.edu.cn (X. Wang))

† These authors contributed equally to this work.

### 1.2 Characterization of NiCoP/g-$C_3N_4$ nanocomposites

The crystal structure of the samples was analyzed using X-ray powder diffraction (XRD, Shimadzu XRD-7000). The surface elemental composition and chemical states were investigated by X-ray photoelectron spectroscopy (XPS, Thermo Fisher Scientific Nexsa G2). The surface morphology of the samples was observed using a scanning electron microscope (SEM, Hitachi S-4800), while the microstructure and detailed morphology were further examined by high-resolution transmission electron microscopy (HRTEM, Thermo Scientific Talos F200X). The optical absorption properties of the NiCoP/CNN nanocomposites were evaluated using UV–visible diffuse reflectance spectroscopy (UV–vis DRS, Cary 5000). The separation efficiency of photogenerated charge carriers was characterized by photoluminescence spectroscopy (PL, F-4700) and time-resolved photoluminescence spectroscopy (TRPL, Edinburgh FLS98).

### 1.3 Photoelectrochemical performance measurement of NiCoP/g-$C_3N_4$ Nanocomposites

The photoelectrochemical (PEC) performance of the samples was evaluated using a CHI-660E electrochemical workstation (Shanghai Chenhua) in a standard three-electrode configuration. A platinum wire was used as the counter electrode, an Ag/AgCl electrode as the reference electrode, and fluorine-doped tin oxide (FTO) glass coated with the photocatalyst served as the working electrode. The electrolyte consisted of 0.1 M $Na_2SO_4$ aqueous solution. A 300 W xenon (Xe) lamp equipped with a UV cut-off filter ($\lambda > 400$ nm) was used as the light source. To prepare the working electrode, 5.00 mg of the sample was ultrasonically dispersed in a mixed solution containing 800 μL isopropanol, 200 μL deionized water, and 40 μL Nafion solution to form a homogeneous suspension. The resulting suspension was then uniformly drop-cast onto the surface of FTO glass (effective area ~2 $cm^2$) and dried at room temperature prior to PEC measurements.

### 1.4 Calculation of apparent quantum efficiency (AQE) of hydrogen evolution

The apparent quantum efficiency (AQE) of $H_2$ evolution was investigated under different monochromatic lights ($\lambda$ = 420, 450 and 550 nm). It was calculated by the following equation.

$$\mathrm{AQE} = \frac{2 \times \text{Number of evolved } H_2 \text{ molecules}}{\text{Number of incident photons}} \times 100\%$$

## 2. Results and Discussion

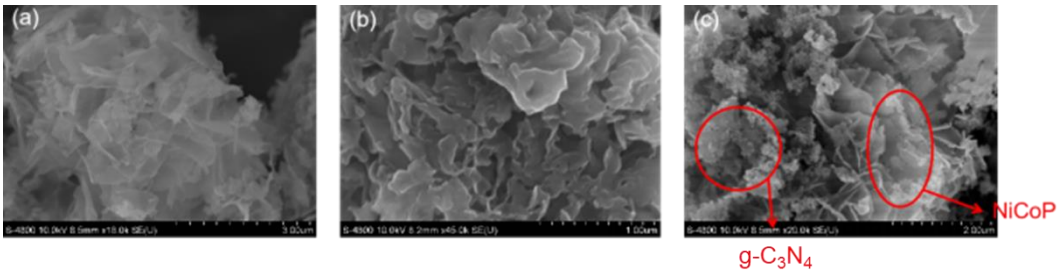


**Figure S2** SEM images: (a) NiCoP; (b) g-$C_3N_4$; (c) NiCoP/g-$C_3N_4$.

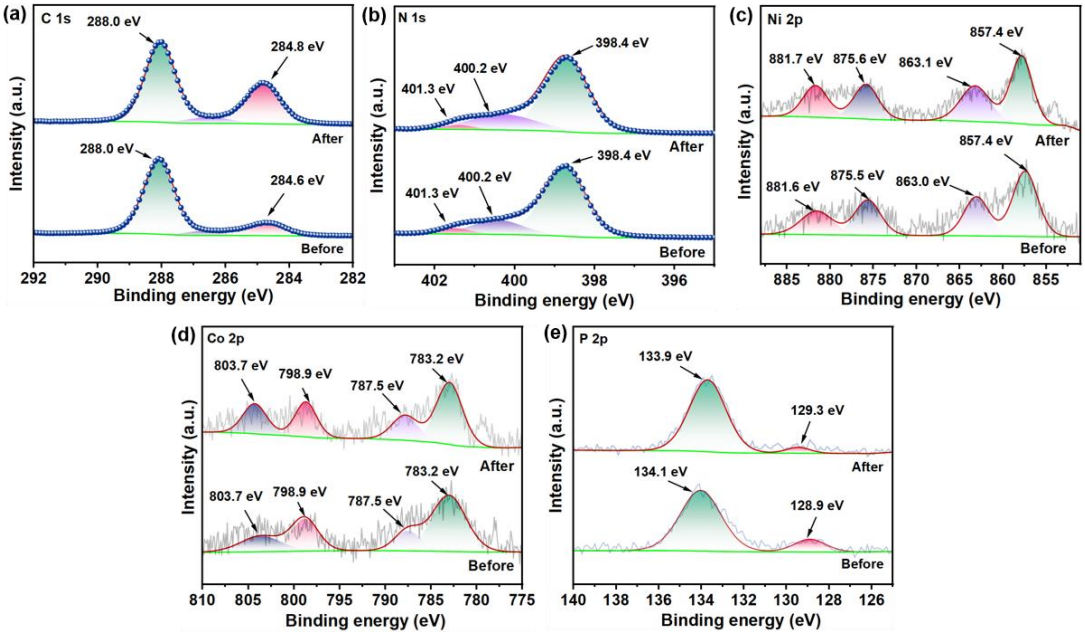


**Figure S3** XPS high resolution spectra of fresh and used 20% NiCoP/g-$C_3N_4$ heterojunction: (a) C 1s; (b) N 1s; (c) Ni 2p; (d) Co 2p; (e) P 2p.

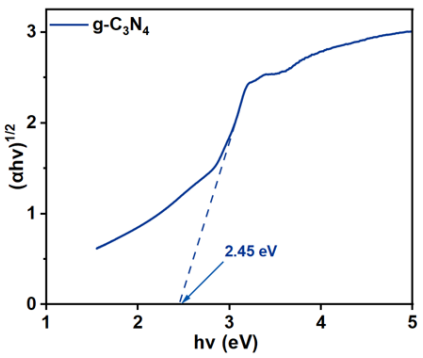


**Figure S4** The band gap of g-$C_3N_4$.

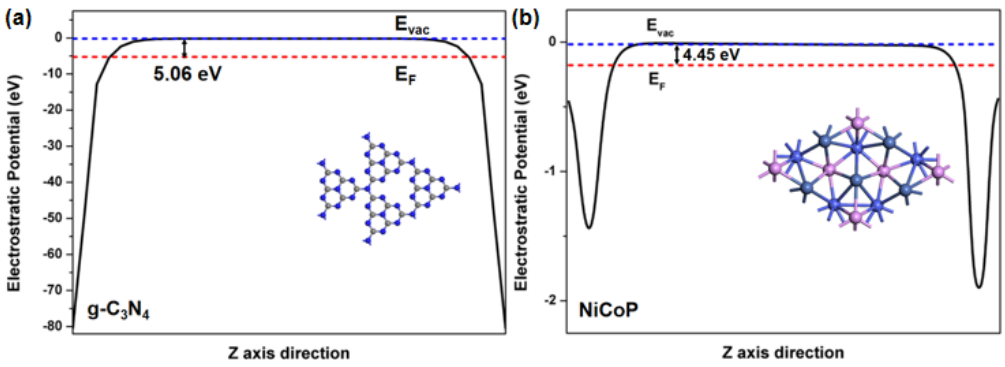


**Figure S5** The work function of (a) g-$C_3N_4$ and (b) NiCoP.

**Table S1** Comparison of the $H_2$ revolution rates with other photocatalysts.

| Photocatalysts | Light source | Sacrificial reagent | Seawater source | $H_2$ evolution rate ($\mu mol \cdot g^{-1} \cdot h^{-1}$) | Refs. |
|---|---|---|---|---|---|
| NiCoP/g-$C_3N_4$ | 300 W Xe lamp ($\lambda \geq 400$ nm) | 10 vol.% TEOA | NSW | 1290.0 | Our work |
| NiCoP/g-$C_3N_4$ | 300 W Xe lamp ($\lambda \geq 400$ nm) | 10 vol.% TEOA | 3 wt% NaCl | 1827.4 | Our work |
| ZCS/CNN | 300 W Xe lamp ($\lambda \geq 400$ nm) | 10 vol.% TEOA | ASW | 726.5 | [1] |
| CCTO/CNT | 420 W Xe lamp | 4 vol.% TEOA | Seawater | 580 | [2] |
| H-CoS/CdS | $\lambda \geq 420$ nm | $Na_2S + Na_2SO_3$ | ASW | 143.1 | [3] |
| $Fe_2O_3$/C-$TiO_2$ | 300 W Xe lamp ($\lambda \geq 420$ nm) | -- | NSW | 170.8 | [4] |
| Z-scheme $Na_2Ti_3O_7$/Ag/CdS | 300 W Xe lamp ($\lambda \geq 420$ nm) | $Na_2S + Na_2SO_3$ | ASW | 1793 | [5] |
| CNv-mCN-Br | 300 W Xe lamp ($\lambda \geq 420$ nm) | TEOA + 1 wt% Pt | ASW | 34.4 | [6] |
| $In_2S_3$/$In_2O_3$ nanosheets | 5 W Blue-LED light ($\lambda = 420$ nm) | 0.1 M L-ascorbic | ASW | 618 | [7] |
| Pt/o-g-$C_3N_4$ | Simulated solar light | Glucose | NSW | 847 | [8] |
| Brookite $TiO_2$ | Full solar spectrum | -- | ASW | 1476 | [9] |

Note: ASW referred to simulated seawater and NSW referred to nature seawater.

**Table S2** The fitting results of the EIS spectra of pure g-$C_3N_4$, pure NiCoP, 20%NiCoP/g-$C_3N_4$ and 25%NiCoP/g-$C_3N_4$ nanocomposites.

| Samples | Rs ($\Omega \cdot cm^2$) | CPE-T ($\Omega^{-1} \cdot cm^{-2} \cdot s^{-n}$) | CPE-P | R1 ($\Omega$-$cm^2$) |
|---|---|---|---|---|
| g-$C_3N_4$ | 26.80 | $4.5362 \times 10^{-5}$ | 0.83473 | 12228 |
| NiCoP | 28.36 | $12.1990 \times 10^{-5}$ | 0.81937 | 13321 |
| 20% NiCoP/g-$C_3N_4$ | 26.62 | $3.8797 \times 10^{-5}$ | 0.83977 | 9128 |
| 25% NiCoP/g-$C_3N_4$ | 27.59 | $9.1754 \times 10^{-5}$ | 0.85165 | 11553 |

## References


[1] Q. Xiao, Y. Fan and L. Zhou, *et al.*, Construction of bimetallic sulfide/carbon nitride nanocomposites for photocatalytic hydrogen evolution from simulated or natural seawater, *J. Photoch. Photobio. A*, 2026, **472**, 116810.

[2] N. Chanda, B. Jaksani and S. Saha, *et al.*, $CaCu_3Ti_4O_{12}$/CNT nanocomposite for enhanced photocatalytic seawater splitting to hydrogen generation, *Int. J. Hydrogen Energ.*, 2025, **140**, 36-44.

[3] S. Liu, Y. Ma and D. Chi, *et al.*, Hollow heterostructure CoS/CdS photocatalysts with enhanced charge transfer for photocatalytic hydrogen production from seawater, *Int. J. Hydrogen Energ.*, 2022, **47**, 9220-9229.

[4] Y. Yang, L. Liu and Q. Qi, *et al.*, A low-cost and stable $Fe_2O_3$/C-$TiO_2$ system design for highly efficient photocatalytic $H_2$ production from seawater, *Catal. Commun.*, 2020, **143**, 106047.

[5] G. Xiong, S. Shen and S. Xiao, *et al.*, Well-defined Z-scheme $Na_2Ti_3O_7$/Ag/CdS multidimensional heterojunctions with enhanced $H_2$ production from seawater under visible light, *Int. J. Hydrogen Energ.*, 2022, **47**, 30503-30516.

[6] M. Guo, M. Chen and J. Xu, *et al.*, C, N-vacancies and Br dopant co-enhanced photocatalytic $H_2$ evolution of g-$C_3N_4$ from water and simulated seawater splitting, *Chem. Eng. J.*, 2023, **461**, 142046.

[7] Y. R. Lin, Y. C. Chang and F. H. Ko. One-pot microwave-assisted synthesis of $In_2S_3$/$In_2O_3$ nanosheets as highly active visible light photocatalysts for seawater splitting, *Int. J. Hydrogen Energ.*, 2024, **52**, 953-963.

[8] A. Speltini, A. Scalabrini and F. Maraschi, *et al.*, Improved photocatalytic $H_2$ production assisted by aqueous glucose biomass by oxidized g-$C_3N_4$, *Int. J. Hydrogen Energ.*, 2018, **43**,

14925-14933.

[9] J. Zhang, Y. Lei and S. Cao, *et al.*, Photocatalytic hydrogen production from seawater under full solar spectrum without sacrificial reagents using $TiO_2$ nanoparticles, *Nano Res.*, 2022, **15**, 2013- 2022.